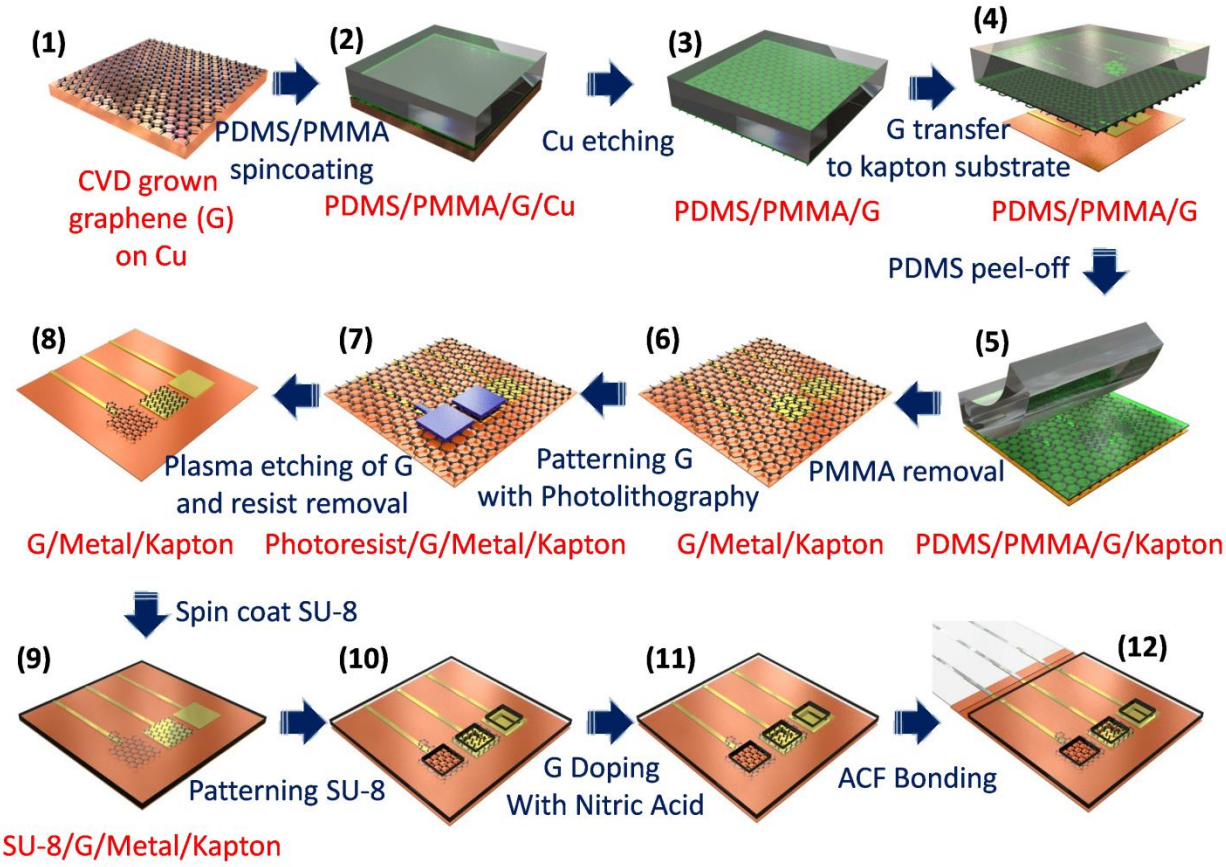

Supplementary Figure 1: Schematic illustrating the fabrication process. Details of fabrication are given in the Methods part. The fabrication process is shown for three different types of electrodes: graphene (G), graphene/gold(G/Au) and gold(Au).

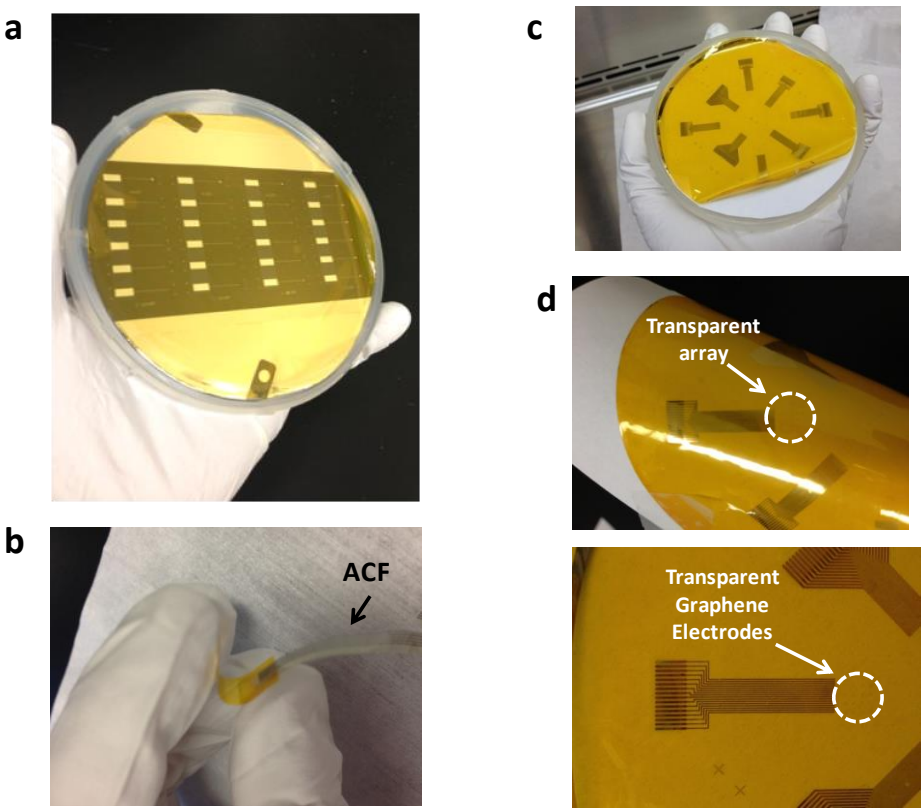

Supplementary Figure 2: a) Single G, G/Au and Au electrodes, fabricated on polyimide substrate using a 4inch Si wafer. **b)** Single G electrode after boding contact pads to flexible ACF cable. Bonding to ACF was performed by applying heat and pressure. **c)** Transparent ECoG arrays after polyimide peel off from the Si carrier wafer. **d)** Top: Transparent arrays can wrap around curvilinear surfaces. Bottom: Gold pads and wires connected to completely transparent 16 electrode array. Faded squares are the electrodes.

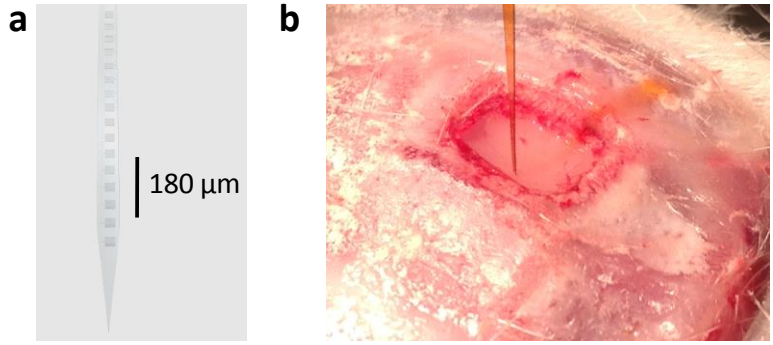

Supplementary Figure 3: a) Schematic explaining transparent penetrating array. **b)** Penetration of kapton is mechanically tested in rat cortex. Penetration width is ~1.5 mm, thickness of kapton was 50 µm the width close to penetrating tip is < 50 µm and close to top is ~100 µm.

Supplementary Figure 4: Cortical EEG recorded by graphene electrode *in vivo* in cat model.

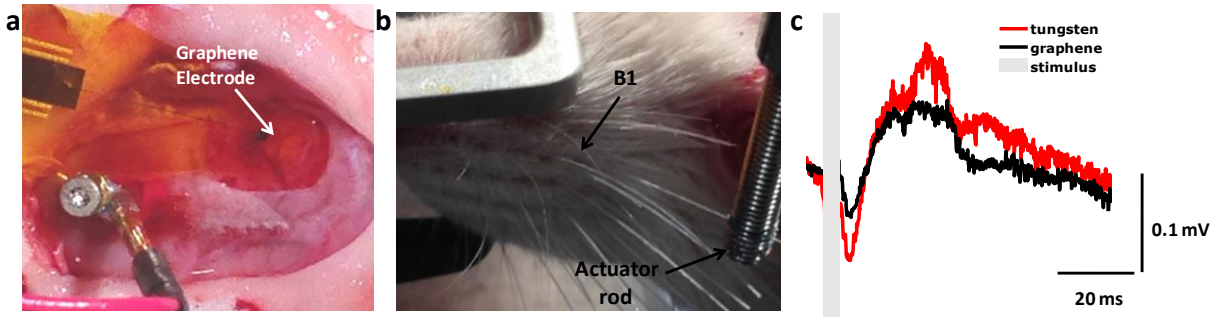

Supplementary Figure 5: Somatosensory evoked potential (SSEP) experiment *in vivo* in anesthetized rats. **a.** 250-µm graphene electrode was placed on the surface of the exposed barrel cortex to record the SSEPs produced by vibrissa (whisker) stimulation. **b.** Left B1 vibrissa was cut to a length of 15mm and attached to the end of an actuator rod. **c.** The figure shows the median of 30 SSEPs recorded with each type of electrode. The gray bar indicates the approximate timing and duration of the mechanical stimulus.

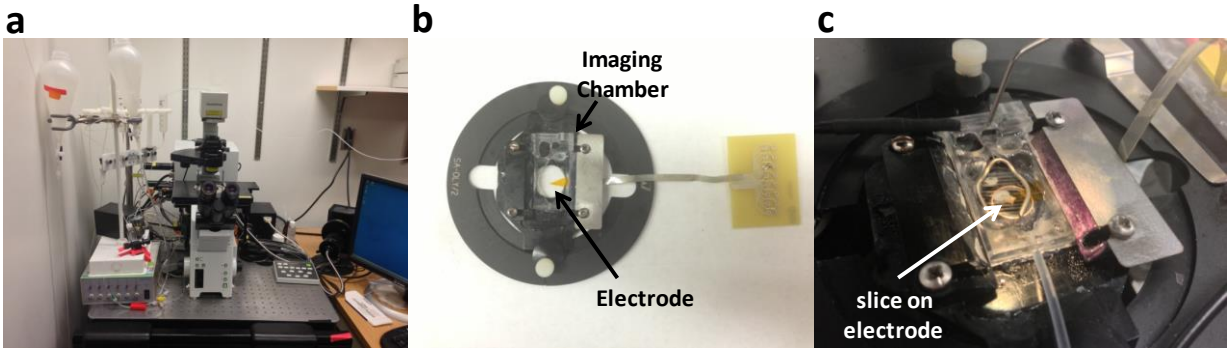

Supplementary Figure 6: a) Confocal microscope setup **b)** Insulating chamber built to submerge and constantly perfuse slices placed at the top of the electrode. **c)** Hippocampal slice placed on the electrode during calcium imaging and neural recording experiments.

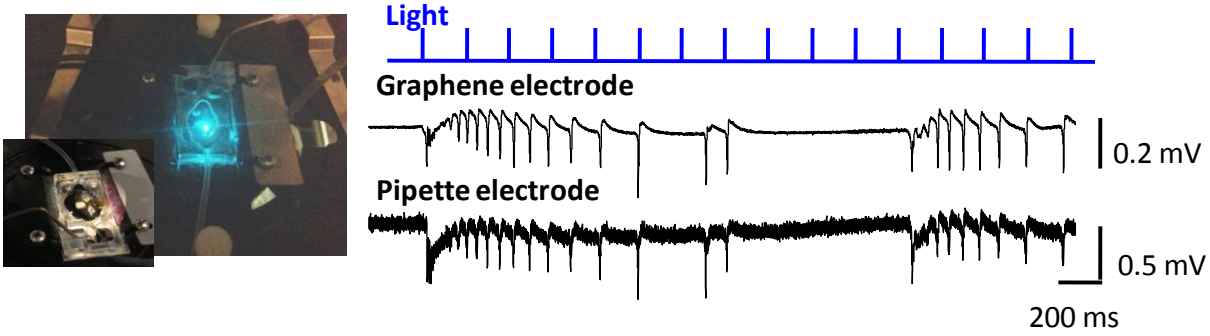

Supplementary Figure 7: a) Excitation laser was illuminated on transparent graphene electrode and hippocampal slice at 5 Hz. A standard glass pipette was also placed close to graphene electrode. Recordings by graphene electrode do not exhibit any light induced artifacts as well as recordings by glass pipette electrode (as expected since glass has no photoelectric effect).

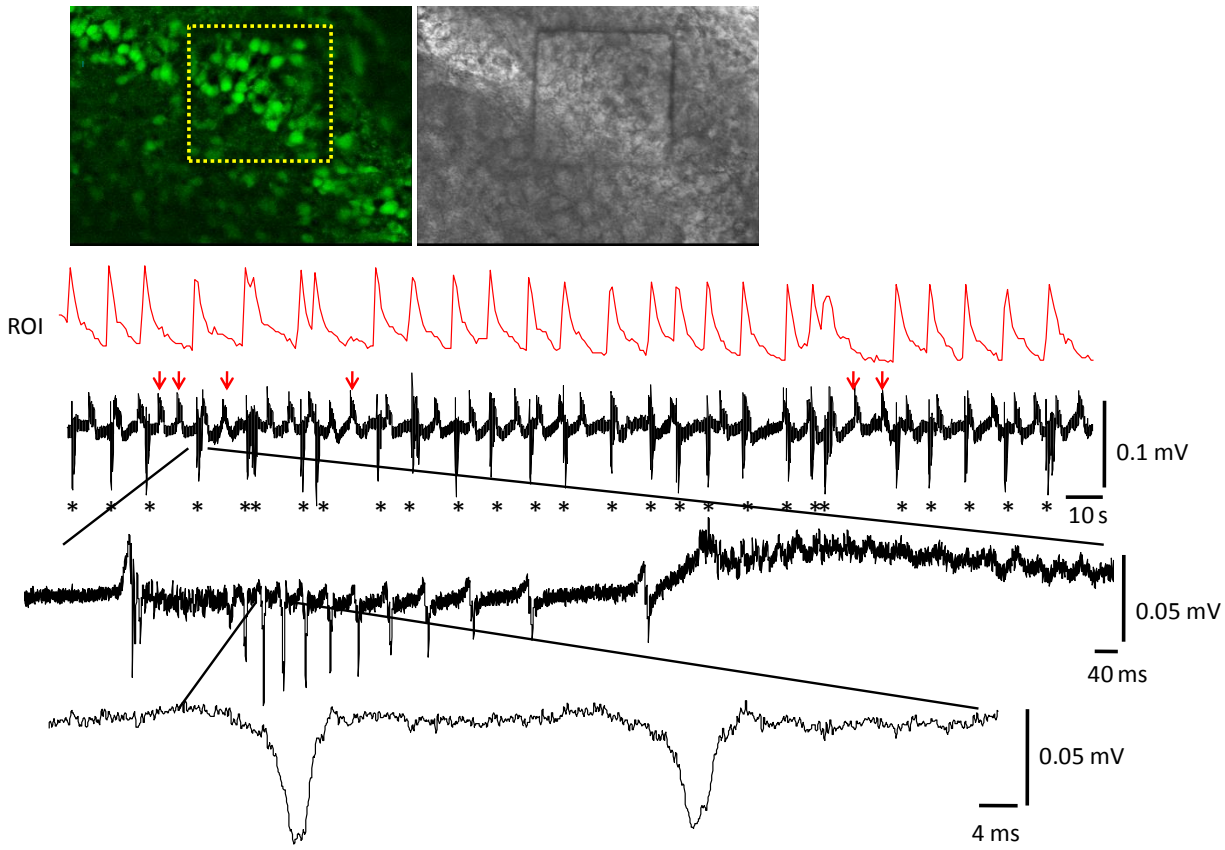

Supplementary Figure 8: Multi-cellular calcium imaging and simultaneous electrophysiology recording from the transparent graphene electrode. **a**, (left) A steady-state fluorescence (F0) image of dentate gyrus obtained by confocal microscopy of a hippocampal slice stained with the calcium indicator OGB-1 AM. The excitation light at 488nm as well as fluorescence emission (max at ~520nm) penetrated through the transparent electrode (graphene and polyimide substrate). (right) Simultaneously obtained transmittance image by the confocal microscopy. It clearly shows the edge of the insulating layer, indicating that the slice and the electrode are in close proximity. Calcium transient (ΔF/F0) for the electrode area (labeled as ROI) shows that an increase in calcium signal coincide with the population activity recorded by the graphene electrode. Zoomed traces show that the graphene electrode was able to measure very fast population spikes with durations less than 5 ms. Red arrows show slow synaptic potentials

recorded by the graphene electrode. Those were not detectable by multi-cellular calcium imaging.

Supplementary Figure 9: Top trace shows the recordings by graphene electrode and the bottom trace shows recordings by a standard patch pipette placed close to the edge of the graphene electrode. Ictal-like activity recorded simultaneously by the graphene electrode and the patch electrode was found to be consistent.

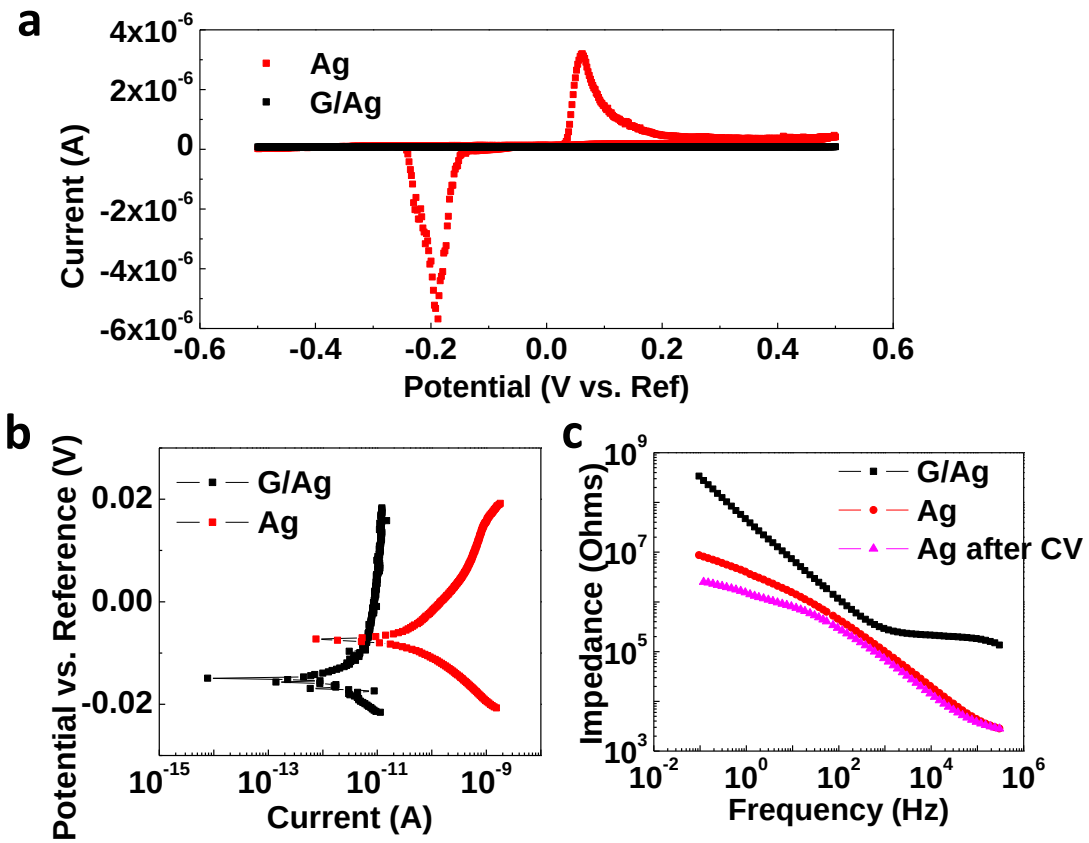

Supplementary Figure 10: a) Cyclic voltammetry for Ag and G/Ag electrodes. Ag curve exhibits two big reaction peaks while G/Ag curve seems like a flat line without any peaks. **b)** Potentiodynamic polarization curves for Ag and G/Ag electrodes. G/Ag has significantly lower corrosion current. **c)** Electro chemical impedance spectroscopy measurement results for Ag, G/Ag and Ag after CV measurements. As a result of faradaic reactions taking place during cyclic voltammetry sweeps, the impedance of Ag electrode significantly decreases at low frequencies.

	Equivalent circuit notion	Equation for impedance	Unit
Solution resistance	R_S	R_S	Ω
Constant phase element	C_{PE}	$\frac{1}{Q(j\omega)^n}$	$S \times s^n$
Charge transfer resistance	R_{CT}	R_{CT}	Ω
Porous bounded Warburg Element	Z_W	$\frac{1}{W_0\sqrt{j\omega}}\tanh(B\sqrt{j\omega})$	$S \times s^{1/2}$
Bounded Warburg Element	Z_W	$\frac{1}{W_0\sqrt{j\omega}}\coth(B\sqrt{j\omega})$	$S \times s^{1/2}$

Supplementary Table 1. Equations for the equivalent circuit model.

Supplementary Note 1: Electrochemical Characterization

To investigate the electrical characteristics of the electrode/electrolyte interface, we used the equivalent circuit model given in Fig. 2 d, where R_S is the solution resistance, C_{PE} is a constant phase element representing the double layer capacitor, R_{CT} is faradaic charge transfer resistance and Z_W is a Warburg element for diffusion. Equations for the equivalent circuit elements are listed in Supplementary Table I. Measured EIS results were fitted to equivalent circuit model to calculate the fit parameters for Au and doped_G electrodes. Porous bounded Warburg element was used to model the diffusion for Au electrode, while bounded Warburg element was used for doped_G electrode because it provided a better fit.

Methods for Somatosensory Evoked Potential Experiment

The following procedures were approved by the Institutional Care and Use Committee of the University of Pennsylvania. One Sprague-Dawley rat was anesthetized with a ketamine (60 mg/kg), xylazine (5 mg/kg) solution and placed in a stereotaxic frame. A craniotomy was performed to expose the right barrel cortex. A skull screw was placed in the right frontal bone to serve as the reference electrode for the recordings.

Mechanical stimulation of the mystacial vibrissae was performed with a linear actuator (LCA8, SMACInc). The left B1 vibrissa was cut to a length of 15mm and attached to the end of the actuator rod with Vetbond adhesive. Each stimulus produced by the actuator caused a 1-mm displacement of the vibrissa in the dorsoventral direction. The stimuli were presented at 0.33 Hz.

Two different types of working electrodes were sequentially placed on the surface of the exposed barrel cortex to record the SSEP produced by the vibrissa stimulation: a 127-μm tungsten electrode and a 250-μm graphene electrode. In initial recordings, the electrode was moved to find the maximum SSEP. Subsequently, each electrode was placed at this optimal location. Stimulus-triggered blocks of data were recorded on a neurophysiology workstation (ZC16, PZ2, RZ2, Tucker-Davis Technologies), which filtered the neural signal with a 0.35 Hz to 7.5 kHz passband and digitized the signal at 6104 Hz. The figure shows the median of 30 SSEPs recorded with each type of electrode. The gray bar indicates the approximate timing and duration of the mechanical stimulus.